Engineering characterization of near fault ground motions

Paul G. Somerville

URS Corporation, Pasadena, CA, USA.

ABSTRACT: Near-fault ground motions are different from ordinary ground motions in that they often contain strong coherent dynamic long period pulses and permanent ground displacements, as expected from seismological theory. The dynamic motions are dominated by a large long period pulse of motion that occurs on the horizontal component perpendicular to the strike of the fault, caused by rupture directivity effects. Forward rupture directivity causes the horizontal strike-normal component of ground motion to be systematically larger than the strike-parallel component at periods longer than about 0.5 seconds. To accurately characterize near fault ground motions, it is therefore necessary to specify separate response spectra and time histories for the strike-normal and strike- parallel components of ground motion. An empirical model for dynamic near-fault ground motions that assumes monotonically increasing spectral amplitude at all periods with increasing magnitude, representing directivity as a broadband effect at long periods, was developed by Somerville et al. (1997). However, near fault recordings from recent earthquakes indicate that the pulse is a narrow band pulse whose period increases with magnitude, causing the response spectrum to have a peak whose period increases with magnitude, such that the near-fault ground motions from moderate magnitude earthquakes may exceed those of larger earthquakes at intermediate periods (around 1 second). A preliminary response spectral model has been developed to incorporate the magnitude dependent shape of the response spectrum of the forward rupture directivity pulse.

1. THE NEAR FAULT RUPTURE DIRECTIVITY PULSE

An earthquake is a shear dislocation that begins at a point on a fault and spreads at a velocity that is almost as large as the shear wave velocity. The propagation of fault rupture toward a site at a velocity close to the shear wave velocity causes most of the seismic energy from the rupture to arrive in a single large pulse of motion that occurs at the beginning of the record, as described by Somerville et al. (1997). This pulse of motion represents the cumulative effect of almost all of the seismic radiation from the fault. The radiation pattern of the shear dislocation on the fault causes this large pulse of motion to be oriented in the direction perpendicular to the fault plane, causing the strike-normal component of ground motion to be larger than the strike-parallel component at periods longer than about 0.5 seconds. To accurately characterize near fault ground motions, it is therefore necessary to specify separate response spectra and time histories for the strike-normal and strike- parallel components of ground motion.

Forward rupture directivity effects occur when two conditions are met: the rupture front propagates toward the site, and the direction of slip on the fault is aligned with the site. The conditions for generating forward rupture directivity effects are readily met in strike-slip faulting, where the rupture propagates horizontally along strike either unilaterally or bilaterally, and the fault slip direction is oriented horizontally in the direction along the strike of the fault. However, not all near-fault locations experience forward rupture directivity effects in a given event. Backward directivity effects, which occur when the rupture propagates away from the site, give rise to the opposite effect: long duration motions having low amplitudes at long periods. The conditions required for forward directivity are also met in dip slip faulting. The alignment of both the rupture direction and the slip direction up-dip on the fault plane produces rupture directivity effects at sites located around the surface exposure of the fault (or its updip projection if it does not break the surface).

The top part of Figure 1 schematically illustrates the orientations of dynamic and permanent near fault ground motions. The strike-slip case is shown in map view, where the fault defines the strike direction. The rupture directivity pulse is oriented in the strike-normal direction and the perma-

nent ground displacement ("fling step") is oriented parallel to the fault strike. The dip-slip case is shown in vertical cross section, where the fault defines the dip direction; the strike direction is orthogonal to the page. The rupture directivity pulse is oriented in the direction normal to the fault dip, and has components in both the vertical direction and the horizontal strike normal directions. The permanent ground displacement is oriented in the direction parallel to the fault dip, and has components in both the vertical direction and the horizontal strike normal direction.

The bottom part of Figure 1 schematically illustrates the partition of near fault ground motions into the dynamic ground motion, which is dominated by the rupture directivity pulse, and the permanent ground displacement. For a strike-slip earthquake, the rupture directivity pulse is partitioned mainly on the strike-normal component, and the permanent ground displacement is partitioned on the strike-parallel component. If the permanent ground displacement is removed from the strike-parallel component, very little dynamic motion remains. For a dip-slip earthquake, the dynamic and permanent displacements occur together on the strike-normal component, and there is little of either motion on the strike-parallel component. If the permanent ground displacement is removed from the strike-normal component, a large directivity pulse remains.

When a near-fault ground motion time history is used for the analysis of a structure at a site, the strike-normal and strike-parallel components need to be oriented with respect to the strike of the fault that dominates the seismic hazard at the site. The strike-normal and strike-parallel components may be transformed into longitudinal and transverse components, preserving the orientation of the motions with respect to the fault strike, as illustrated on the right side of Figure 2.
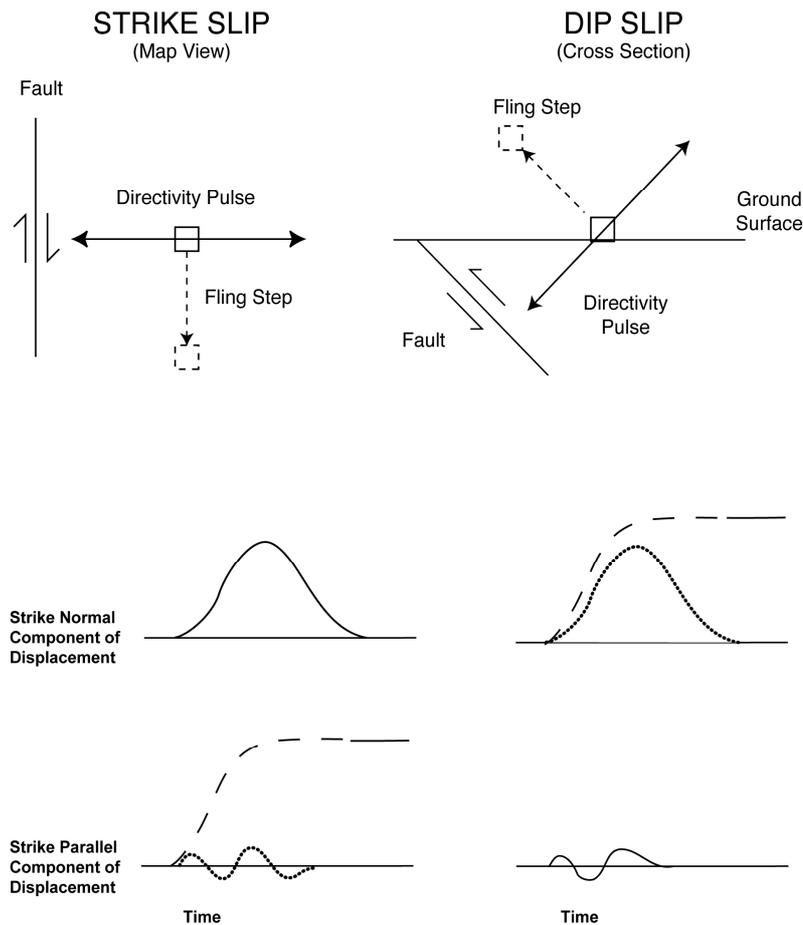

Figure 1. Top: Schematic orientation of the rupture directivity pulse and fault displacement ("fling step") for strike-slip (left) and dip-slip (right) faulting. Bottom: Schematic partition of the rupture directivity pulse and fault displacement between the strike normal and strike parallel components of ground displacement. Waveforms containing static ground displacement are shown as dashed lines; versions of these waveforms with the static displacement removed are shown as dotted lines.
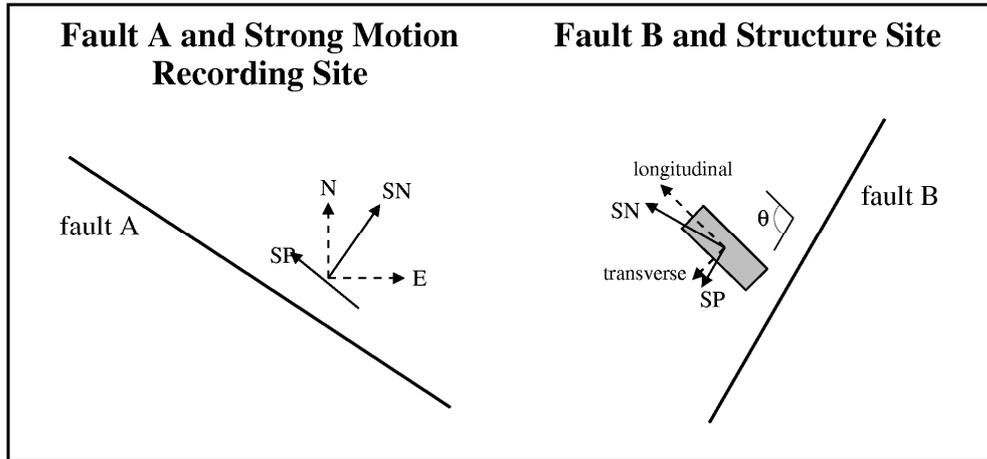
Figure 2. Archiving (left) and application (right) of strike-normal and strike-parallel components of ground motion.

2 NEAR FAULT GROUND MOTION MODELS

The relationships between the dynamic and permanent components of near-fault ground displacements are quite complex, as illustrated in Figure 1. For example, the rupture directivity pulse and the permanent ground displacement occur on orthogonal components in strike-slip faulting, but on the same component in dip-slip faulting. The rupture directivity pulse can be very strong off the end of a strike-slip fault, where there is little or no permanent displacement. The 1989 Loma Prieta and 1994 Northridge earthquakes produced strong rupture directivity pulses even though they did not rupture the ground surface. This indicates that separate models are needed for predicting the dynamic and permanent components of near-fault ground displacements at a site. The separately estimated dynamic and permanent components of the ground motion can be combined to produce ground motion time histories representing both effects. In the following, we present models for predicting dynamic near fault ground motions. The permanent displacement field of earthquakes can be calculated using theoretical methods (e.g. Aki and Richards, 1980), and surface fault displacements can be estimated using empirical models (e.g. Wells and Coppersmith, 1994).

2.1 Broadband Directivity Model

A model that can be used to modify conventional ground motion attenuation relations to account for the amplitude and duration effects of rupture directivity was developed by Somerville et al. (1997). This model was modified by Abrahamson (2000) to incorporate a directivity saturation effect and to taper it at small magnitudes and large distances. In this model, amplitude variations due to rupture directivity depend on two geometrical parameters. First, the smaller the angle between the direction of rupture propagation and the direction of waves traveling from the hypocenter to the site, the larger the amplitude. Second, the larger the fraction of the fault rupture surface that lies between the hypocenter and the site, up to a limit of 40% of the fault length, the larger the amplitude. Attenuation relations modified to include directivity effects can be used directly in probabilistic seismic hazard analysis (PSHA), as described by Abrahamson (2000). The parameters that control rupture directivity effects are the location and orientation of the fault rupture plane, and the location of the hypocenter on the rupture plane. The directivity model is implemented in PSHA by randomizing the location of the hypocenter on the fault planes of earthquakes having magnitudes larger than 6.

2.2 Magnitude Scaling of Response Spectra of Near Fault Ground Motions

Strong motion recordings of the recent large earthquakes in Turkey and Taiwan confirm that the near fault pulse is a narrow band pulse whose period increases with magnitude. The recent earthquakes also have surprisingly weak ground motions at short and intermediate periods (0.1 to 3.0 seconds), weaker than those of smaller (magnitude 6 ¾ - 7.0) earthquakes (Somerville, 2003). These ob-

servations require reevaluation of the magnitude scaling in current models of near fault ground motions and in current source scaling relations (Somerville et al., 1997, 1999).

In Figure 3, rupture directivity pulses of earthquakes in the magnitude range of 6.7 to 7 are compared with pulses from earthquakes in the magnitude range of 7.2 to 7.6. The narrow band nature of these pulses causes their elastic response spectra to have peaks, as shown in Figure 4. The fault-normal components (which contain the directivity pulse) are shown as solid lines, and the fault-parallel components, which as expected are much smaller at long periods, are shown by long dashed lines. The 1994 UBC spectrum for soil site conditions is used as a reference model for comparison. The fault-normal spectra for the large earthquakes (right column) are compatible with the UBC code spectrum in the intermediate period range, between 0.5 and 2.5 seconds, but have a bump at a period of about 4 seconds where they significantly exceed the UBC code spectrum. The fault-normal spectra of the smaller earthquakes (left column) are very different from those of the larger earthquakes. Their spectra are much larger than the UBC code spectrum in the intermediate period range of 0.5 - 2.5 sec, but are similar to the UBC spectrum at longer periods.
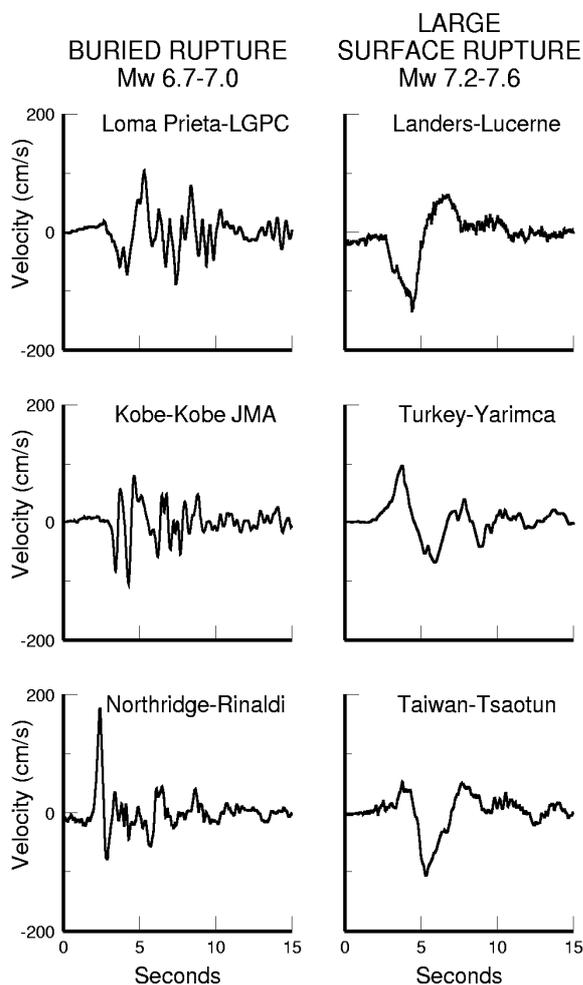

Figure 3. Fault-normal velocity pulses recorded near three moderate magnitude earthquakes (left column) and three large magnitude earthquakes (right column), shown on the same scales.

The magnitude scaling exhibited in the data in Figures 3 and 4 is contrary to current models of earthquake source spectral scaling and ground motion spectral scaling with magnitude, including Somerville et al. (1997), which assume that spectral amplitudes increase monotonically at all periods. However, these magnitude scaling features are the natural consequence of the narrow band character of the forward rupture directivity pulse. The period of the near fault pulse is related to source parameters such as the rise time (duration of slip at a point on the fault) and the dimensions of asperities on

the fault that produce coherent long period ground motions, which generally increase with magnitude (Somerville, 1998). Near fault ground motions cannot be adequately described by uniform scaling of a fixed response spectral shape, because the shape of the intermediate and long period part of the fault-normal response spectrum changes as the level of the spectrum increases and as the magnitude increases.
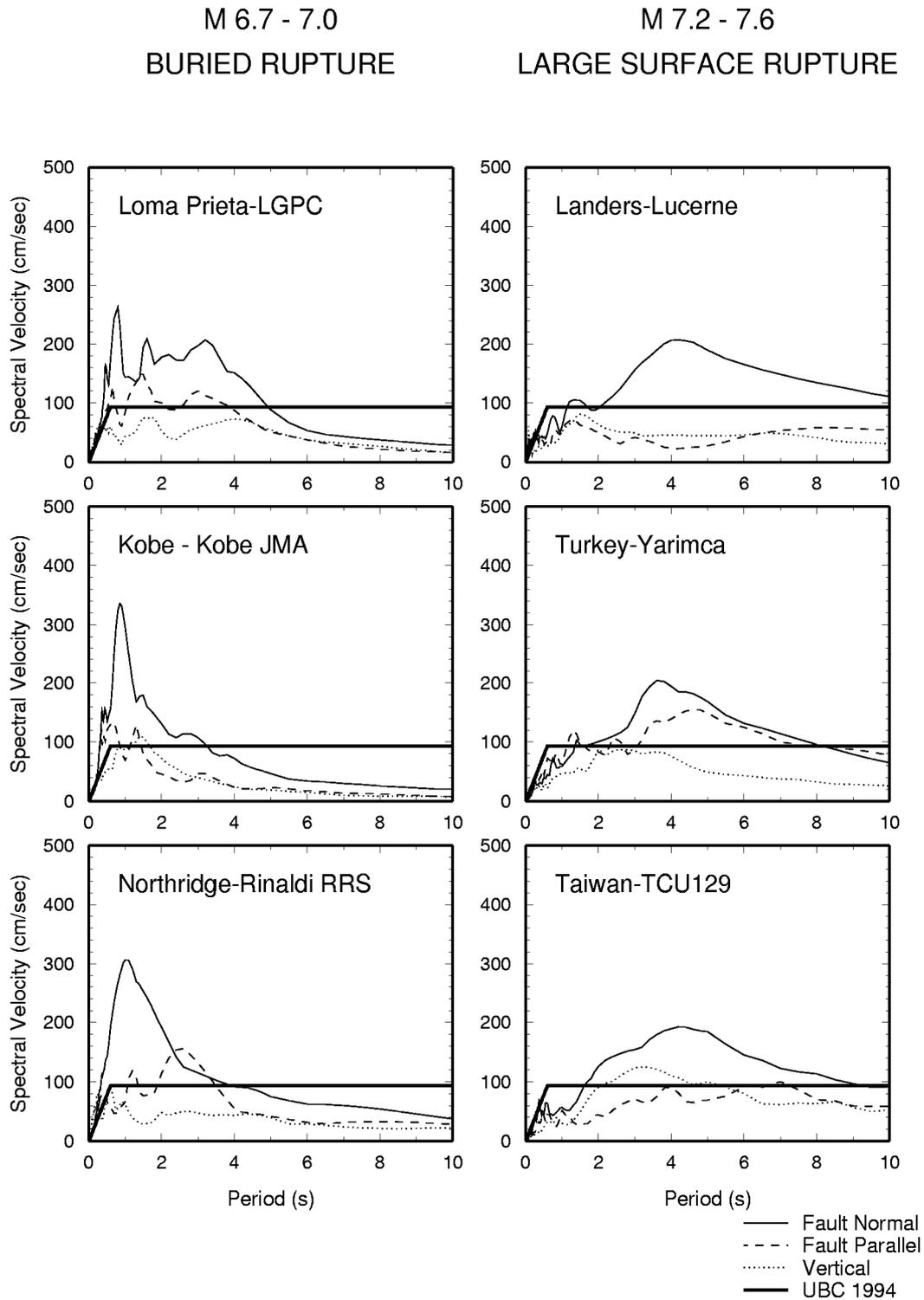
M 6.7 - 7.0
BURIED RUPTURE

M 7.2 - 7.6
LARGE SURFACE RUPTURE

Figure 4. Spectral velocity of fault-normal pulses of moderate (left) and large (right) earthquakes.

2.3 Magnitude Scaling of the Forward Rupture Directivity Pulse

To augment these response spectral models of near fault ground motions, time domain models of the forward rupture directivity pulse have been developed. Near fault ground motions containing forward rupture directivity are often simple enough to be represented by simple time domain pulses, thus simplifying the specification of ground motion time histories for use in nonlinear structural response analyses. Equations relating the period and amplitude of the fault-normal forward rupture directivity velocity pulse to earthquake magnitude and distance have been developed by Somerville (1998), Somerville et al. (2000), Alavi and Krawinkler (2000), Rodriguez-Marek (2000), and Mavroeidis and Papageourgiou (2003).

Somerville (2003) updated the relationship between velocity pulse period and magnitude using data from the 1999 Chi-Chi, Taiwan and Kocaeli, Turkey earthquakes. Separate relationships were developed for near fault recordings on rock and soil sites. These relationships use the period T_{Dir} of the largest cycle of the fault-normal velocity waveform recorded at stations near the fault that experience forward rupture directivity. The recordings used were mostly within 10 km of the fault, and the period was assumed to be independent of the distance from the fault. These empirical relationships are defined only for full forward rupture directivity conditions, and are not defined for the full range of angles and rupture distances that are included in the Somerville et al. (1997) response spectral model for rupture directivity effects. The data for rock are consistent with a self-similar scaling relationship in which the period of the pulse T_{Dir} increases in proportion to the fault length. This is consistent with the self-similar nature of the source scaling relations found by Somerville et al. (1999). The relationship is: $\log10 T_{Dir} = -3.17 + 0.5 M_W$

The response spectral characteristics of fault-normal velocity pulses whose periods follow the magnitude scaling characteristics described above are illustrated in Figure 5. Simple triangular velocity pulses whose period scaling with magnitude follows the above relation for rock and whose amplitude scaling follows Somerville (1998) are shown on the left side, and the corresponding elastic acceleration and velocity response spectra are at the center and right. The elastic response spectra have peaks that are related to the period of the pulse. For spectral acceleration, the period of the peak is about 0.75 times the period of the velocity pulse, and for spectral velocity, the peak is at about 0.85 times the period of the pulse. Because of these peaks, and because the peak velocity of the pulse does not increase very rapidly with magnitude, the response spectra do not increase monotonically with magnitude at all periods, as is the case in conventional ground motion models. Instead, the response spectra of smaller earthquakes are stronger than the response spectra of larger earthquakes in some period ranges. These features are similar to those seen in the data shown in Figures 3 and 4.
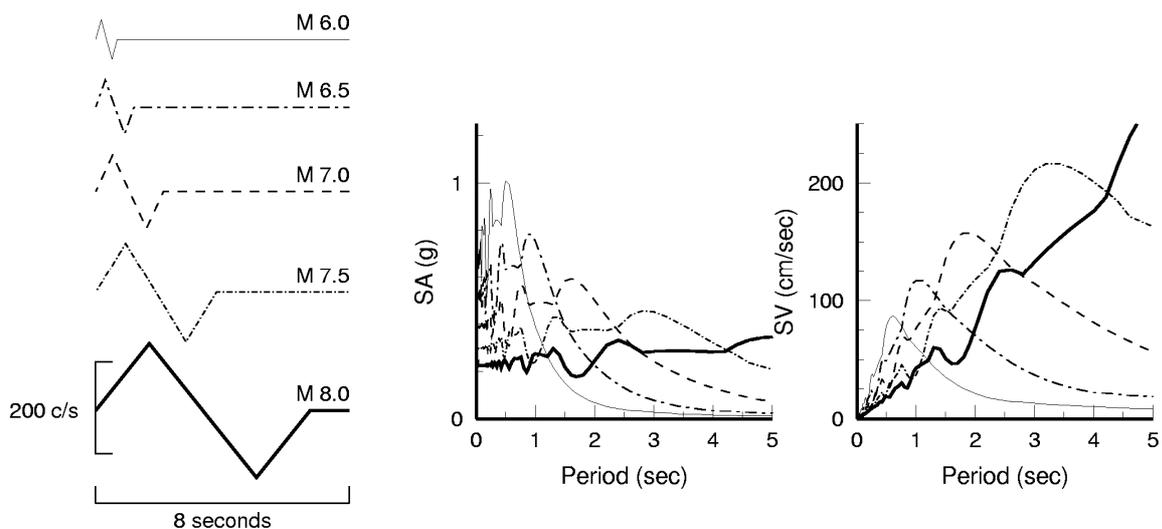

Figure 5. Magnitude scaling of simple velocity pulses representing near fault ground motions (left) and their acceleration (center) and velocity (right) response spectra.

2.4 Narrow Band Rupture Directivity Model

We have developed preliminary response spectral models that include the magnitude dependence of the period of the rupture directivity pulse, derived from the relations between pulse period and magnitude given above. This response spectral model is for the horizontal fault-normal component under maximum rupture directivity conditions ($X\cos\theta = 1$ in Somerville et al. (1997). A conventional acceleration response spectrum is assumed to represent the fault-parallel component. To obtain the response spectrum of the fault-normal component, the fault-parallel response spectrum is scaled by a cosine-shaped function centered at a period equal to 0.75 times the value of T_{Dir} of the velocity pulse for a given magnitude M_w from the equation given above. We found that a peak amplitude of 2 for the scaling function (with a standard error of 0.4 natural log units), and a width of about a factor of 1.5 on either side of $T_{Dir,}$, are consistent with the data . The average horizontal component is obtained by using a scaling function with a peak amplitude of the square root of 2.

In Figure 6, we compare the fault-normal response spectra for rock and soil predicted by this narrow band model with the standard model of Abrahamson and Silva (1997), which does not explicitly include directivity effects, and the broadband model of Somerville et al. (1997), whose directivity effects are based on the monotonic increase of ground motion amplitudes with magnitude at all response spectral periods. The new models produce larger response spectra in the period range of about 0.5 to 2 seconds for earthquakes smaller than M_W 7.5, and smaller response spectra at all periods for earthquakes larger than M_W 7.5, compared with the Somerville et al. (1997) model.

REFERENCES:

Abrahamson. N.A. and W.J. Silva, 1997. Empirical response spectral attenuation relations for shallow crustal earthquakes. *Seismological Research Letters*, 68: 94-127.

Abrahamson, N.A., 2000. Effects of rupture directivity on probabilistic seismic hazard analysis. Proceedings of the 6th International Conference on Seismic Zonation, Palm Springs, Earthquake Engineering Research Institute.

Aki, K. and P.G. Richards (1980). *Quantitative Seismology: Theory and Methods*. W.H. Freeman & Co.

Alavi, B. and H. Krawinkler, 2000. Design considerations for near-fault ground motions. *Proceedings of the U.S. – Japan Workshop on the Effects of Near-Fault Earthquake Shaking*, San Francisco, March 20-21.

Mavroeidis, G. and A. Papageourgiou, 2003. A mathematical representation of near fault ground motions. *Bull. Seismol. Soc. Am. 93,* 1099-1131.

Rodriguez-Marek, A., 2000. Near fault seismic site response. Ph.D. Thesis, Civil Engineering, University of California, Berkeley, 451 pp.

Somerville, P.G., N.F. Smith, R.W. Graves, and N.A. Abrahamson (1997). Modification of empirical strong ground motion attenuation relations to include the amplitude and duration effects of rupture directivity, *Seismological Research Letters* 68, 199-222.

Somerville, P.G., K. Irikura, R. Graves, S. Sawada, D. Wald, N. Abrahamson, Y. Iwasaki, T. Kagawa, N. Smith and A. Kowada (1999). Characterizing earthquake slip models for the prediction of strong ground motion. *Seismological Research Letters*, 70, 59-80.

Somerville, P.G. (1998). Development of an improved representation of near fault ground motions. Proc. SMIP98 Seminar on Utilization of Strong Ground Motion Data, p. 1-20.

Somerville, P.G., H. Krawinkler and B. Alavi, 2000. Development of improved ground motion representation and design procedures for near-fault ground motions. *Final Report to CSMIP Data Utilization Program*, Contract No. 1097-601.

Somerville, P.G. (2003). Magnitude scaling of the near fault rupture directivity pulse. Physics of the Earth and Planetary Interiors, 137, 201-212.

Wells, D.L. and K.J. Coppersmith (1994). Analysis of empirical relationships among magnitude, rupture length, rupture area, and surface displacement, *Bull. Seismol. Soc. Am. 84,* 974-1002.
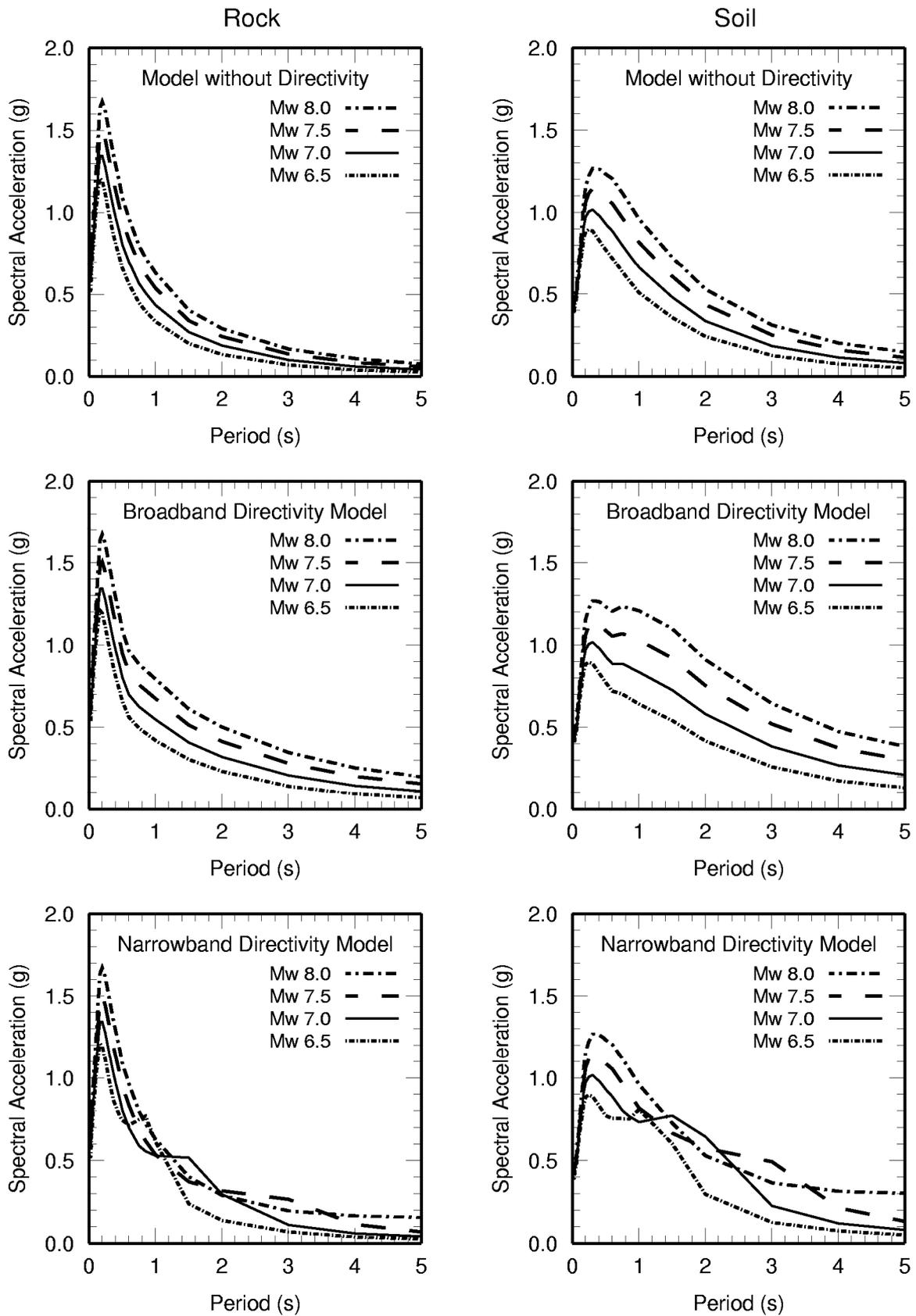
Figure 6. Near fault response spectral model, strike-slip 5km for rock sites (left) and soil sites (right). Top: model without directivity (Abrahamson and Silva, 1997). Middle: Broadband directivity model (Somerville et al, 1997). Bottom: Narrow band directivity model (Somerville, 2003).